

Effective Slab Width Model for Seismic Analysis of Flat Slab Frames

by Laurel M. Dovich and James K. Wight

An effective slab width model is developed to describe the lateral behavior of a reinforced concrete flat slab frame within a two-dimensional nonlinear frame analysis. The parameters of the model are based on experimental data from a two-story, two-bay flat slab frame tested under cyclic lateral loads. The model is useful for estimating the strength and stiffness of a flat slab frame either for the design of new structures or for economic seismic retrofit of older flat slab structures. The simplicity and usefulness of the model is demonstrated by a pushover analysis, which post-predicted observed earthquake damage to a slab-column frame. For a four story building with a stiff perimeter beam-column frame, the pushover analysis indicated that the interior slab-column frame carried a significant amount of the total base shear.

Keywords: effective width; flat slab; frame.

INTRODUCTION

Flat slab structures are used extensively due to the economy of the structural system and the architectural versatility. The behavior and design of flat slab structures for gravity loads are well established. Their behavior under lateral displacements, however, is not well understood and lateral design methods are not well established. Transfer of lateral displacement-induced moments at slab-column connections is a complex three-dimensional behavior, consisting of flexure, torsion, and shear stresses in the slab around the periphery of column faces. Slab shear stresses caused by moment transfer are added to the gravity shear stresses at the connection. When the combined shear stresses become too large, a brittle punching failure will occur. If the connections are not properly detailed, punching failure may lead to progressive collapse.

Currently, codes allow the use of flat slab structural systems to resist wind and seismic forces in low and moderate seismic zones. Due to its flexibility, the flat slab must be combined with a stiffer lateral force resisting system in high seismic regions. The flat slab system must be able to drift with the lateral moment resisting system, however, and thus still requires special attention for lateral loadings. For typical frame structures, the flat slab frame has significant lateral stiffness, and thus attracts some load due to lateral displacements. If the connections do not have enough strength to transfer these lateral loads, local failures could result. Thus, estimating the lateral stiffness and strength of the flat slab frame is important for the design of new structures and for economic seismic retrofit of older flat slab structures. Finite element analysis could be used for this estimation, but requires excessive computational time and computer resources even for relatively small problems. Also, the output from finite element analysis is not as compatible with reinforced concrete design as the output from frame analysis. Thus, attempts have been made to model the properties of

slab-column behavior as a two dimensional frame. Two approaches have been used: torsional member methods and effective slab width methods.

The most common torsional member method is the Equivalent Column Method, developed originally for gravity loads¹ and adapted for lateral loads.² It defines a transverse torsional spring to model the torsional stiffness of the slab adjacent to the slab-column connection. This stiffness is combined with column stiffness to give properties of an equivalent column. This model is inconvenient to implement in typical two-dimensional elastic frame programs, and is generally only applied to single story, two-dimensional slab strips. This method has been adopted into the ACI Building Code (ACI 318-02).³

The effective slab width method models the slab as a beam, so it is easily used with frame analysis software. The equivalent width of the slab-beam element is adjusted to simulate the actual behavior of the three-dimensional system, while the depth remains the actual depth of the slab. The effective width accounts for the behavior of the slab that is not fully effective across its transverse width.

Effective slab widths were initially defined analytically by matching the model response to elastic plate theory and finite element analysis of a slab-column connection. More recent proposals for effective slab widths are calibrated to match experimental behavior of laterally-loaded slab-column systems. Many of the experimental results have been from isolated connections, which do not have the redundancy and moment redistribution capabilities of a full frame. The proposed models have obtained good correlations, but they are cumbersome and not readily adopted for use in a design office.

Research has identified parameters that affect the effective slab width in determining strength and stiffness of the model: the aspect ratio of the columns and panels,⁴ the type of connection (that is, interior, exterior, corner, edge)⁵⁻⁷, the level of gravity load,^{6,7} differing negative moment and positive moment response,⁸ the amount of initial cracking,⁵ and the presence of a drop panel.⁹ For all of these proposed models, it is difficult to account for the degradation of member and connection stiffness due to increased lateral drift while using an elastic analysis. Grossman⁵ and Robertson⁸ targeted their effective slab width models to match the experimental data at several discrete drifts. Whereas, Luo and Durrani^{6,7} proposed using an equivalent moment of inertia I_e based on M_d/M_{cr} at each loading level.

ACI Structural Journal, V. 102, No. 6, November-December 2005.

MS No. 04-321 received October 6, 2004, and reviewed under Institute publication policies. Copyright © 2005, American Concrete Institute. All rights reserved, including the making of copies unless permission is obtained from the copyright proprietors. Pertinent discussion including author's closure, if any, will be published in the September-October 2006 *ACI Structural Journal* if the discussion is received by May 1, 2006.

ACI member **Laurel M. Dovich** is a professor of engineering at Walla Walla College, College Place, Wash. She is former Chair of ACI Committee 120, History of Concrete, and is also a member of ACI Committee E 802, Teaching Methods and Educational Materials. Her research interests include seismic behavior, design of reinforced concrete, teaching reinforced concrete design, and historic concrete structures.

James K. Wight, F.A.C.I., is a professor of civil engineering at the University of Michigan, Ann Arbor, Mich. He is Chair of ACI Committee 318, Structural Concrete Building Code, and is a member of Joint ACI-ASCE Committees 352, Joints in Monolithic Concrete Structures, and 445, Shear and Torsion. His primary research interests include earthquake-resistant design of reinforced concrete structures and the use of high-performance fiber-reinforced cementitious composites in critical members or regions of such structures.

Experimental research¹⁰ has documented that inelastic behavior occurs in flat slab frames at low drifts. Connection yield was observed at 0.75% drift and slab flexural cracking occurred long before that. This indicates that an inelastic analysis, which accounts for stiffness degradation with drift, is more appropriate than an elastic analysis for modeling these structures.

The effective slab width model proposed here provides a simple methodology for lateral load analysis of flat slab systems. It uses a nonlinear analysis that incorporates stiffness degradation to better describe the actual behavior of the frame under lateral loads. The parameters of the model are based on measured and observed data from a two-story, two-bay slab-column frame, which includes redundancies for redistribution of the loads. When used in a nonlinear push-over analysis, this model enforces lateral drift compatibility between the slab-column frame and the lateral load resisting system, so loss of stiffness and damage to the slab-column can be evaluated. Incorporating the stiffness of the slab-column frame in the structural system should improve the economy of new construction and seismic retrofit schemes.

RESEARCH SIGNIFICANCE

This paper presents a simple effective slab width model for slab-column frames that is conducive to efficient use in a design office. The model is useful for estimating the lateral strength and stiffness of flat slab frames, either for the design of new structures or for economic retrofit of older flat slab

structures. Data from a pushover analysis using this model can identify the drift at which punching shear would be expected, thus dictating the stiffness needed for the lateral force resisting system in high seismic regions.

DEVELOPMENT OF EFFECTIVE SLAB WIDTH MODEL

The effective slab width model was developed to match the strength and stiffness of a 1/3-scale experimental two-story, two-bay reinforced concrete flat slab frame specimen, configured as shown in Fig. 1. It was detailed according to the practices of the 1960s and early 1970s, meaning most significantly that the bottom steel was discontinuous at the connections. Standard drop panels were incorporated at the connections, but no special shear reinforcing was used. No torsional element or spandrel beam was used along the exterior perimeter of the slab. The specimen carried a gravity load that provided an average of $0.064\sqrt{f'_c}$ MPa ($0.77\sqrt{f'_c}$ psi) shear stress on the critical shear section of an interior connection. The specimen was subjected to quasi-static reversed cyclic loading, with drifts increasing in increments of 0.25%, up to a maximum drift of 2%. For more detailed information on the experimental specimen, refer to Dovich and Wight.^{10,11} The effective slab width model was developed using data from strain gauges attached to the slab reinforcement, and matching measured strength and stiffness of the frame.

Due to variation in depth of the slab and drop panels, the effective slab-beam for each span was comprised of three segments, a middle segment, and drop panel segments at both ends, as shown in Fig. 2(a). The three segments were connected to form the effective slab-beam element. Separate effective slab-beam elements were developed for the interior and exterior spans, because different behavior was observed in each span. Also, strength and stiffness properties were considered separately to model the behavior of the slab-beam as accurately as possible.

Strength model

Interior drop panel—To define the effective width for moment participation across the slab at an interior connection,

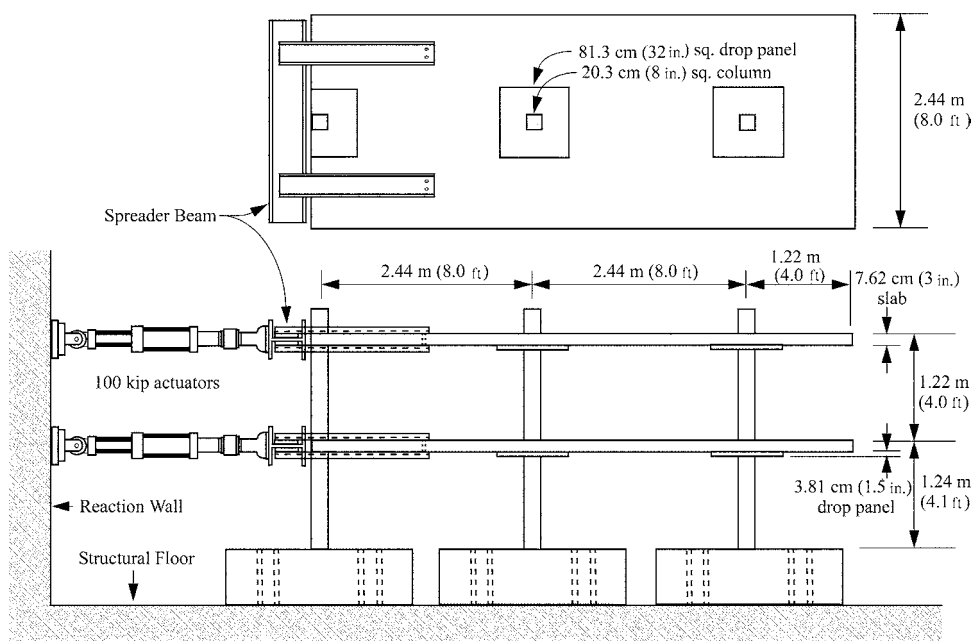


Fig. 1—Two-story, two-bay frame test setup.

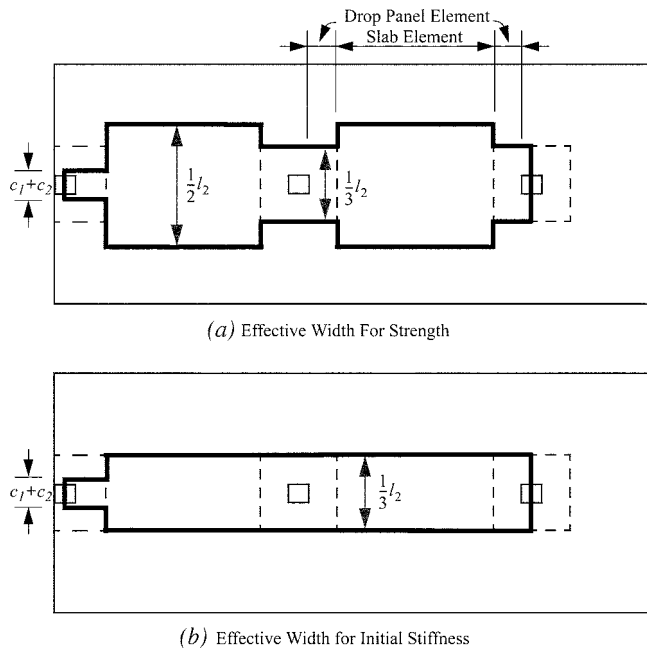


Fig. 2—Effective slab widths for strength and stiffness.

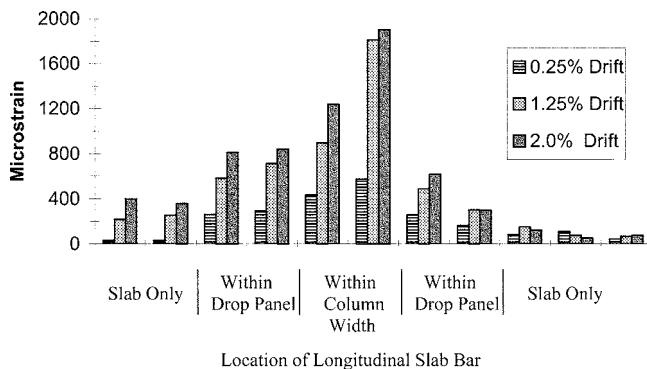


Fig. 3—Measured strain range per cycle in top longitudinal bars across transverse width of slab.

strain gauges were placed on the top slab bars across the transverse width of the two-story, two-bay frame specimen, in line with the transverse face of the column. Half were positioned transversely on the side of the column where tension strains would be expected in the top reinforcement for positive lateral displacements. The other half were positioned along a line parallel to the opposite face of the same column, and thus were expected to experience compression strains due to positive lateral displacements. More details on the experimental aspects can be found in Dovich and Wight.^{10,11}

Slab participation was evaluated from the working strain, defined as the total strain difference measured between the positive displacement peak and the negative displacement peak of the same cycle. As seen in Fig. 3, there was not a completely symmetric distribution of working strain on either side of the interior column. It is clear, however, that the working strains drop off for slab bars located farther from the column. A notable drop in working strains occurred beyond the drop panel. Based on this data, the effective slab width for flexural strength at an interior connection was defined as the width of the drop panel ($l_2/3$).

Exterior drop panel—At the exterior connections, torsional cracks, which initially appeared at average drifts of

1.0%, essentially isolated the outer portions of the slab from the column. These cracks opened at approximately 45 degrees to the column side faces. Based on this observation and strain gauge data, the effective width at exterior connections was taken as the column width plus half of the total column depth on each side ($c_1 + c_2$). This assumes that slab bars within the inner half of the torsional crack do effectively transfer moment to the column. The effective width was observed to increase away from the column face, but was kept constant for strength analysis as shown in Fig. 2(a).

Midspace—Away from the connections, a larger portion of the slab contributed to the positive flexural resistance of the slab. Therefore, for the middle portion of the slab-beam element, the effective width for strength was defined as half of the transverse span of the slab ($l_2/2$). Figure 2(a) shows the segments and effective slab widths assumed for the flexural strength of the slab-beam elements in the two-story, two-bay frame.

Verification of strength effective width model—frame strength calculations

The proposed effective slab width strength model was verified by comparing analytical strength calculations to the measured strength of the two-story, two-bay frame. A virtual work analysis was performed in which the lateral loads at the floor levels were proportioned to be at the same ratio as the experimental lateral load distribution at 2% average drift for both directions of lateral displacement. The unknown lateral loads were solved for, assuming plastic hinging action at the base of the columns and in the slab at the column faces. Strength capacities of the model at the locations of these zero-length plastic hinges were defined to correspond with experimental behavior and the effects of gravity loads were accounted for.

Capacities—The nominal capacities of the slab were based on the flexural strength of the effective widths of Fig. 2(a). The slab and column member strength capacities at the connections were adjusted as shown in Table 1. In locations where strain gauge data did not show full yield at 2% drift, 80% of M_n was assumed to be a good representation of the capacity. Because of the additional effective depth at the drop panels, both layers of slab bars were considered to be in tension for the calculated negative moment capacity.

The column strength was defined as the nominal moment capacity from its interaction diagram, taking the gravity load on the columns into account. It was assumed that at 2% drift the nominal interaction diagram was appropriate to use, as opposed to the yield diagram.

Accounting for gravity load—The amount of slab moment capacity that is available for resisting lateral displacement-induced moments is the excess moment capacity not used in resisting gravity loads. This lateral moment capacity was taken as the nominal capacity of the section effective width (or 80% of the nominal capacity as defined in Table 1) minus the estimated gravity moment at the connection.

The initial gravity moment distribution was estimated by strain gauge readings under gravity loads only, and corresponded to theoretical strains for a calculated moment of $wl^2/12$ at the centerline of an interior column. Testing showed, however, that this initial moment would rapidly be redistributed after a couple lateral displacement cycles due to a loss of stiffness at the connections, and was evidenced by positive moment cracking at midspace. Thus, the exact gravity moment distribution could not be explicitly defined.

For continuous interior connections, the magnitude of the gravity moment is not an issue. To define the net lateral moment capacity of an interior connection, the gravity moment is subtracted from the negative nominal capacity on one side of the column, and added to the positive nominal capacity on the other side of the column, thus cancelling out its overall effect.

Due to the discontinuity of the experimental frame, however, gravity moment did affect the second interior connection of the two-story, two-bay frame, where there was no lateral moment resistance from the discontinuous slab to offset the addition or subtraction of gravity moment. To account for moment redistribution due to a loss of stiffness at the connections, 25% of the initial gravity moment was used at this discontinuous interior connection.

At the exterior span, recommendations from Section 13.6.3.3 of ACI 318-02³ were used to allocate the gravity moments. The lack of flexural cracks in the bottom of the slab at midspan indicated that there was not a large redistribution of gravity moments in this span.

Verification—Using the lateral load distribution observed experimentally at 2% drift and the strength capacities of the interior and exterior connections as given in Table 1 (adjusted for gravity moments), a virtual work analysis was used to solve for the magnitude of the total lateral strength of the frame. In Table 2, the measured forces for each lateral displacement direction are compared with the forces calculated from the proposed effective slab width model. The predicted lateral force, based on the stated effective widths, effective capacities, and gravity moment redistributions, was 10 to 15% smaller than the measured force. The effect of axial loads within the redundant frame and strain hardening of the reinforcement could account for the differences between predicted and measured forces.

Calibration of stiffness effective width

Experimental data indicated yielding in the flat slab frame at 0.75% drift, preceded by flexural cracking at lower drift levels. Thus, an inelastic analysis is much more appropriate than an elastic analysis for lateral loads, even at low drifts. For the proposed model, effective widths are established to describe the initial lateral stiffness of the frame. The model is put into an analysis program, and stiffness degradation is modeled using nonlinear analysis parameters. This is different than other effective width models⁵⁻⁸ where stiffness at discrete drifts or loads is sought, using an elastic analysis. In Luo and Durrani's model,^{6,7} stiffness degradation was accounted for by calculating an equivalent moment of inertia I_e based on M_a/M_{cr} at each load level. In Robertson's model,⁸ adjustment factors are used to describe stiffness degradations at 1/2% and 1-1/2% drift.

The initial stiffness of the experimental frame was modeled by using plane frame analysis with the slab-beam moment of inertia based on trial effective widths for stiffness. The moment of inertia of the effective widths was reduced to reflect softening caused by flexural cracking due to gravity load. The reductions taken were those commonly used in practice, that is, $I_g/3$ for the slab and $3I_g/4$ for the columns.

The model for initial stiffness was calibrated by analytically subjecting the effective slab width model of the two-story, two-bay frame to the gravity and lateral loads applied to the experimental specimen at the positive and negative peaks of the first cycle (0.25% drift), which was essentially an elastic cycle. Lateral displacements were calculated for these loads,

Table 1—Member capacities used in virtual work analysis

Location		Assumed percentage of nominal capacity of effective width	Reason
Slab—exterior connection	Negative capacity	100%	Mechanism developed
	Positive capacity		
Slab—interior connection	Negative capacity	80%	Strain gauge data did not show full yield at 2% drift
	Positive capacity		
Column		100%	Yield strains measured

Table 2—Comparison of strength model calculations to experimental measurements

Second floor actuator force, kN (kip)	Measured (2.0% drift)	Calculated from effective width model
Positive lateral displacement	61.4 kN (13.8 kip)	54.3 kN (12.2 kip)
Negative lateral displacement	52.9 kN (11.9 kip)	46.3 kN (10.4 kip)

Table 3—Experimental and calculated story stiffness

Initial stiffness, kN/mm (kip/in.)	Positive displacement		Negative displacement	
	Top floor	Bottom floor	Top floor	Bottom floor
Experimental	7.15 (40.8)	12.5 (71.5)	5.99 (34.2)	11.8 (67.1)
Calculated	5.32 (30.4)	14.6 (83.5)	5.01 (28.6)	15.3 (87.6)

based on the described model. Effective slab widths were adjusted until the calculated displacements approximately matched the applied displacements.

The slab effective width for stiffness at the drop panels was assumed to be the width of the drop panel ($l_2/3$), because the additional depth gives it much more flexural stiffness than the adjoining slab. At midspan, a good fit with the measured stiffness was obtained with an effective width of $l_2/3$, as shown in Fig. 2(b). Similar to the strength model, the slab effective width for stiffness narrows down at the exterior connection due to flexural-torsional cracks that isolated the connection from the outer portions of the slab. For analysis, the column width plus half of the total column depth on each side ($c_1 + c_2$) was used as the effective width for the exterior drop panel.

The effective story stiffnesses calculated with this analytical model are compared to the initial measured stiffnesses in Table 3. The experimental value is the secant stiffness from zero to peak displacement of the first cycle (0.25% drift). The model consistently predicts stiffnesses that are higher than the experimental values for the bottom floor, and lower than the experimental values for the top floor. Overall, the theoretical model, which was not adjusted from story to story, was assumed to give a good estimate of the initial stiffness of the two-story structure.

Summary of slab-beam model

The strength and stiffness modeling parameters are summarized in Table 4. Different effective slab widths are given for the drop panel zone adjacent to the connection and middle segments for the span. The drop panel elements extend over the length of the drop panel. The proposed effective slab width model satisfactorily predicted the behavior of the two-story, two-bay frame, and thus should apply to any other flat slab frame with the same general configuration and levels of gravity loads. It must be noted that this model does

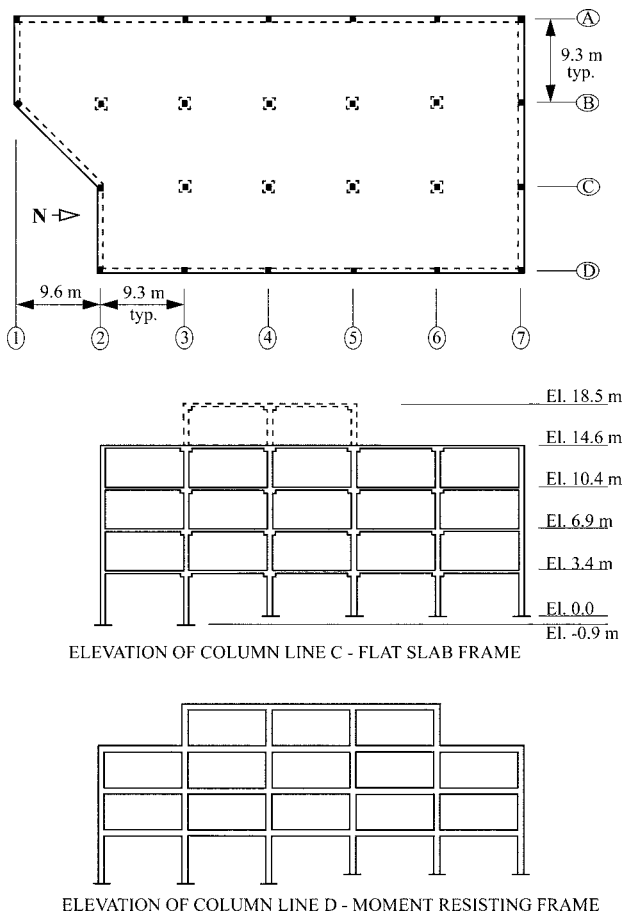


Fig. 4—Office building first-floor plan and two superstructure frame elevations.

not account for failure by punching shear nor loss of anchorage of discontinuous bottom bars. It is intended to give an estimate of the strength and stiffness contributions of a flat slab frame at relatively low drift levels.

Discontinuous bottom bars

If the positive moment reinforcement is discontinuous through the connection, as in older construction, it could lose anchorage before gaining the full moment capacity of the effective width. In a separate test of an isolated interior slab-column connection with discontinuous bottom bars, anchorage was lost at 1.5% drift.^{10,11} Up to this point the positive capacity was only equal to the cracking strength of the slab section. Beyond this drift, the only net positive capacity was the unloading of the negative gravity moment at the connection.

During the testing of an isolated exterior connection with unanchored bottom reinforcement, the reinforcement did not slip until between 2.0 and 3.0% drift.¹⁰ The drift level at which loss of anchorage occurred indicates that a portion of the nominal positive capacity could be used if drifts were controlled. The effective width at the exterior connection, however, is very narrow, and the contribution from the positive nominal capacity over this width would not be large enough to greatly affect the strength of the frame as a whole.

APPLICATION OF EFFECTIVE SLAB WIDTH MODEL

The proposed effective slab width model was used to simulate the behavior of a slab-column office building (Fig. 4)

Table 4—Proposed effective slab widths

Effective widths	Drop panel element*		Midspan slab element
	Exterior connection	Interior connection	
Strength	$c_1 + c_2$	$l_2/3$	$l_2/2$
Initial stiffness†	$c_1 + c_2$	$l_2/3$	$l_2/3$

*Include top and bottom reinforcing bars for negative moment capacity calculations.

†Use 1/3 of I_g based on this effective width to account for cracking.

that experienced punching shear failures during the Northridge earthquake (1994). The lateral force was expected to be resisted by the stiffer exterior moment resisting frame, and compatible drift requirements of the interior slab-column frame were probably not fully taken into account. The office building did not have high gravity loads at the time of the earthquake, so the observed punching failures in the slab-column frame are attributed to displacement-induced moments being transferred by eccentric shear stresses at the interior connections. A push-over analysis was performed to see if the stiffness of the interior flat slab connections attracted enough moment to cause a failure in punching shear. The availability of this office building data provided a means of testing the proposed effective slab width model and demonstrated the value of performing a static push-over analysis at the design stage.

A pushover analysis consists of pushing the building analytically in one direction by incrementally increasing lateral loads until it reaches a specified drift. An inelastic structural analysis program originally developed by Kanaan and Powell¹² and modified by Tang and Goel,¹³ was used for the pushover analysis. The slab-column frame was modeled by the effective slab width model proposed here. The data from the pushover analysis was used to evaluate potential punching shear failure and make other observations about the interaction between the interior slab-column frames and the perimeter beam-column frames.

Modeling the building

The office building, constructed in 1977, was four stories high with a small penthouse on top, as shown in Fig. 4. It was three bays wide in the East-West direction and five to six bays long in the North-South direction. All the columns were 610 mm (24 in.) square. The moment resisting frame around the perimeter had 610 mm wide x 760 mm deep (24 x 30 in.) beams. Steel reinforcement of the members varied with the height of the building. The interior frames consisted of a 220 mm (8-1/2 in.) thick post-tensioned two-way slab with column caps at the connections. These column caps protruded 190 mm (7-1/2 in.) below the slab for a 1.2 x 1.2 m (4 x 4 ft) area at the top of the interior columns. The columns were set on caissons connected by grade beams.

The punching shear failures experienced during the Northridge earthquake are assumed to have resulted primarily from movement in the North-South direction as indicated by recorded ground motions and observed damage to other buildings in the area. Thus, the building was modeled for a static pushover in the North-South direction. The building was represented by a two-dimensional model by treating each column line (in the direction of movement) as a two-dimensional frame. These plane frames were then rigidly linked together to move as a unit. Due to the relative symmetry of the office building, only half the frames in the North-South direction were modeled. The frames used for

Table 5—Differences between experimental and Northridge buildings

Type of difference	Experimental model	Northridge Office Building
Connection geometry	Full drop panel	Small drop panel*
Connection detailing	Discontinuous bottom bars	Continuous bottom bars
Slab reinforcement	Reinforcing bars	Post-tensioned strands
Slab concrete	Normalweight	Sand lightweight
Exterior slab connection	No torsional element	Transverse beam

*Sometimes referred to as column cap.

this analysis were Column Line D, an exterior moment resisting frame, and Column Line C, an interior slab-column frame (Fig. 4). The penthouse on this interior frame was ignored because it was just an enclosure for equipment attached at the roof level.

The slab-column frame of the office building was not identical to the experimental frame discussed earlier. The physical differences between the Northridge office building and the experimental frame are outlined in Table 5. Because of these differences, adjustments had to be made to the effective slab width model. A short explanation of each adjustment follows.

The office building had very narrow drop panels and the effective slab width for moment resistance was expected to be wider than these panels. Also, the in-plane forces due to post tensioning of the slab would result in a wider section of slab resisting moments. Thus, for strength, the full transverse width was considered to be effective for both the drop panel segment of the span and the middle slab segments, which is in agreement with recommendations by Naaman.¹⁴ The office building had the beams of the moment resisting frame around the perimeter, so it was assumed that these beams effectively transferred the slab moments to the column. Thus, the full width of the slab was used for strength calculations at the exterior connections.

For stiffness, the effective slab width was kept at $l_2/3$ for the full span length. It was assumed that the added in-plane compression from post-tensioning would delay cracking and restrict crack openings. To account for this, the cracked moment of inertia was taken as $2I_g/3$ (I_g = gross moment of inertia for $l_2/3$) for negative moment resistance at the slab-column connections. The behavior in positive bending is similar to a non-post-tensioned reinforced concrete section because the post-tensioning strands are placed on the compression side of the neutral axis. Thus, the cracked moment of inertia for positive moment resistance at the slab-column connection was taken as $I_g/3$. A cracked stiffness of $2I_g/3$ was used for the middle portions of the slab, beyond the column cap.

The office structure columns were connected to 9 m (30 ft) long belled caissons, 910 mm (3 ft) in diameter. The interaction of the caissons and the structure was modeled using concepts by Singh, Donovan, and Jobsis.¹⁵ The caissons were modeled as an additional column below the structure, with a length equal to 1/3 of the actual caisson length. These equivalent columns were fixed at their base and restricted from horizontal movement at their top to simulate the effect of the grade beams that were used to tie the caissons together. This approximate model was assumed to be accurate enough for this analysis.

Pushover analysis loading pattern

No standard loading pattern has been established for static inelastic pushover analyses. The building was analytically subjected to both a rectangular and an inverted triangular lateral loading pattern and the response of the structure was dependent on which lateral loading pattern was used. The rectangular pattern consists of an equal load at each story level. The triangular loading, which consisted of higher story loads at the top and lower loads at the lower stories, was distributed according to UBC-97 provisions.¹⁶ The triangular load pattern will maximize the roof drift and overturning moment. Diebold and Moehle¹⁷ noted that at times during their shaketable test of a slab-column structure, the lateral load was uniform over the height. They concluded that this rectangular loading gave an upper bound estimate of the base shear capacity. Thus, triangular and rectangular lateral loading patterns were assumed to represent the extremes of earthquake loading.

Punching shear failure prediction

Because most frame analysis programs do not check for punching shear failures, punching shear stresses were predicted by taking the unbalanced moments at the slab-column connections from the inelastic structural analysis and hand calculating the shear stress v_u on the critical slab section using the ACI 318-02³ eccentric shear stress model. The equation sums the shears generated from gravity load V_u and unbalanced moment M_u as shown below.

$$\frac{V_u}{A_c} \pm \frac{\gamma_v M_u c}{J_c} = v_u \quad (1)$$

where A_c is the area of the concrete critical section; J_c/c reflects the geometric properties of the critical section; and γ_v is the proportion of unbalanced moment transferred by shear (0.4 for square columns).

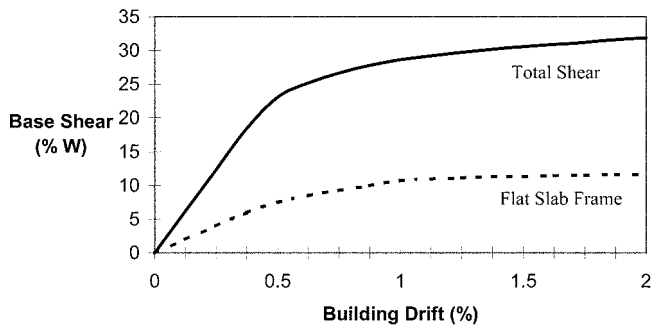
The critical shear section outside the column cap predicted higher shear stresses than the critical shear section around the column. This is consistent with the observed physical damage of the office building, where the punching shear failures occurred outside the column capitals. The shear stresses calculated from Eq. (1) for the slab critical section at an interior connection are given in Table 6 as a multiple of the square root of the slab compressive strength ($f'_c = 27.6$ MPa [4000 psi]). They are based on a superimposed uniform gravity load of 1.92 kN/m² (40 lb/ft²) in addition to the weight of the slab. No load factors were used.

ACI 318-02³ gives three equations in Section 11.12.2.1 for the nominal shear stress. The equation which controls in this case is

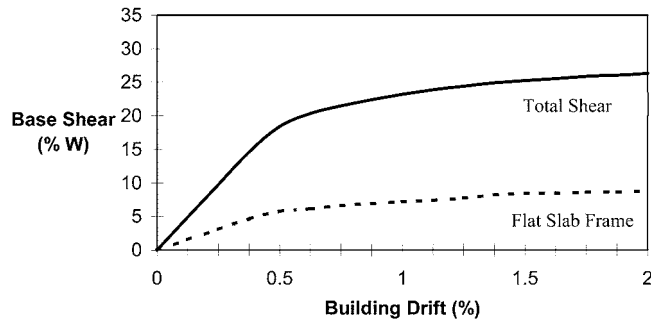
$$v_c = \left(\frac{\alpha_s d}{b_o} + 2 \right) \frac{\sqrt{f'_c}}{12} \quad (2)$$

where b_o is the perimeter of the critical slab section for punching shear; d is the slab effective depth; and α_s is equal to 40 for interior connections.

The value from this equation needs to be reduced by 0.85 to account for the lower shear capacity of sand lightweight concrete. Thus, the nominal shear stress that can be carried by the concrete is 0.208 MPa (2.51 psi).



(a) Rectangular Lateral Loading



(b) Triangular Lateral Loading

Fig. 5—Base shear versus lateral load.

ACI 318-02³ allows an increase in nominal shear stress for pretensioned slabs and the post-tensioned slab modeled here should qualify for this increase. The appropriate equation is given in Section 11.12.2.2.

$$v_c = \beta_p \sqrt{f'_c} + 0.3f_{pc} + \frac{V_p}{b_o d} \quad (3)$$

where β_p is $(\alpha_s d/b_o + 1.5)/12 \leq 0.29$; f_{pc} is the average value of effective prestressing stress for two directions; and V_p is the vertical component of effective prestress forces.

In the Eq. (3), V_p was neglected due to the shallow drape of the post-tensioned strand in the slab, and f_{pc} was calculated on the basis of the column strip width. The nominal shear stress, reduced for sand lightweight concrete, was $0.237\sqrt{f'_c}$ MPa ($2.85\sqrt{f'_c}$ psi).

In comparing the nominal shear stress value of $0.237\sqrt{f'_c}$ MPa to the predicted values in Table 6, a punching shear failure would be predicted between 1.0 and 1.25% drift. Based on damage to other buildings in the area,¹⁸ it is quite certain that the local ground accelerations were high enough to cause a drift of at least 1.25% in this office building. Thus, this analysis demonstrates the value of performing a static pushover analysis at the design stage.

Additional observations

Comparisons between maximum interstory drift and overall building drift, and the sharing of lateral load between the interior slab-column frame and exterior beam-column frame are given here. The pushover analysis did not include the loss of strength and stiffness due to punching failures, so the following observations are accurate for the Northridge office building only up to the drift that punching shear failures were expected (1.0 to 1.25% drift).

Table 6—Predicted shear stresses on critical section

Lateral loading pattern	1.0% drift	1.25% drift	1.5% drift
Rectangular, MPa (psi)	$0.232\sqrt{f'_c}$ ($2.79\sqrt{f'_c}$)	$0.242\sqrt{f'_c}$ ($2.91\sqrt{f'_c}$)	$0.245\sqrt{f'_c}$ ($2.95\sqrt{f'_c}$)
Triangular, MPa (psi)	$0.229\sqrt{f'_c}$ ($2.76\sqrt{f'_c}$)	$0.238\sqrt{f'_c}$ ($2.87\sqrt{f'_c}$)	$0.244\sqrt{f'_c}$ ($2.94\sqrt{f'_c}$)

Table 7—Interstory drifts

Story level	Overall building drift			
	1.0%		1.5%	
	Rectangular	Triangular	Rectangular	Triangular
4	0.66%	0.93%	0.95%	1.41%
3	1.12%	1.20%	1.64%	1.77%
2	1.25%	1.13%	1.84%	1.66%
1	1.04%	0.76%	1.68%	1.17%

Interstory drift—Table 7 gives a comparison between interstory drifts and overall building drift from the office building analysis. It should be noted that the maximum interstory drift is approximately 25% larger than the overall building drift, and thus each connection in the slab-column frame system should have the ability to resist transfer moments caused by drifts that are larger than the expected overall building drift.

Base shear—The base shear versus building drift from the pushover analysis is plotted in Fig. 5. This corresponds to the base shear of the frames along Column Lines C and D (Fig. 4), an interior slab-column frame, and an exterior moment resisting frame. It is interesting to note that the base shear of the flat slab frame accounts for approximately 1/3 of the total base shear for both loading patterns. Because the flat slab resists a significant amount of the base shear, the cost of a retrofit for an older frame structure that does not have sufficient lateral strength could be reduced if this contribution was taken into consideration.

Rectangular versus triangular loading—The plots in Fig. 5 show that there is a significant difference in the lateral strength of the building for the two lateral loading patterns. The rectangular loading pattern achieved higher base shears than the inverted triangular lateral loading pattern because the effective force for the triangular loading is higher up in the building. This creates a larger moment arm, and thus increases the overturning moment for the same base shear. Table 7 shows that interstory drifts tend to be more uniform for triangular lateral loading as compared with rectangular loading.

The lateral load pattern to be used for push-over analysis needs to be studied further. Strength design is conservatively based on the lower bound triangular loading. If force distributions during peak excursions caused by earthquake motions tends to a rectangular distribution, then the lateral load capacity of the building will increase and problems could develop at shear-critical locations within the structure.

CONCLUSIONS

Based on the results of this study, the following conclusions can be drawn:

1. Based on experiments on a two-story, two-bay slab-column frame, modeling rules were established for determining effective slab widths for strength and initial stiffness, as given in Table 4. The exterior connections contribute little to lateral strength and stiffness, as reflected in the small effective

slab widths at that connection. The model is simple and straightforward for design use, and is applicable to conditions similar to those used in this experimental study.

2. Using inelastic analysis software to model the lateral stiffness degradation with increasing drift gave good results at low and high drift levels. It was much less cumbersome than prior models, where adjustments to stiffness need to be made for different load or drift levels.

3. The effective width rules were used to model the lateral load behavior of a four-story reinforced concrete frame structure damaged during the Northridge Earthquake. An inelastic pushover analysis of the building model resulted in a post-prediction of punching shear failures similar to those observed in the actual structure.

4. The results of this study indicate that if an inelastic push-over analysis had been used at the design stage, it could have predicted that slab punching shear was possible at drifts reasonably expected to occur during a moderate to severe earthquake. Even though the exterior moment resisting frame was designed to take the full lateral load, a pushover analysis would have provided a check on the drift capacity of the whole structure.

5. Using the lateral strength and stiffness of existing slab-column frame systems as part of the design of a seismic strengthening plan for an older frame structure can lead to cost savings for the retrofit system.

REFERENCES

1. Corley, W. G., and Jirsa, J. O., "Equivalent Frame Analysis for Slab Design," *ACI JOURNAL, Proceedings* V. 67, No. 11, Nov. 1970, pp. 875-884.
2. Vanderbilt, D. M., "Equivalent Frame Analysis for Lateral Loads," *Journal of the Structural Division*, ASCE, V. 105, No. ST10, Oct. 1979, pp. 1981-1998.
3. ACI Committee 318, "Building Code Requirements for Structural Concrete (ACI 318-02) and Commentary (318R-02)," American Concrete Institute, Farmington Hills, Mich., 2002, 443 pp.
4. Pecknold, D. A., "Slab Effective Width for Equivalent Frame Analysis," *ACI JOURNAL, Proceedings* V. 72, No. 4, Apr. 1975, pp. 135-137.
5. Grossman, J. S., "Verification of Proposed Design Methodologies for Effective Width of Slabs in Slab-Column Frames," *ACI Structural Journal*, V. 94, No. 2, Mar.-Apr. 1997, pp. 181-196.
6. Luo, Y. H., and Durrani, A. J., "Equivalent Beam Model for Flat-Slab Buildings—Part I: Interior Connections," *ACI Structural Journal*, V. 92, No. 1, Jan.-Feb. 1995, pp. 115-124.
7. Luo, Y. H., and Durrani, A. J., "Equivalent Beam Model for Flat-Slab Buildings—Part II: Exterior Connections," *ACI Structural Journal*, V. 92, No. 2, Mar.-Apr. 1995, pp. 250-257.
8. Robertson, I. N., "Analysis of Flat Slab Structures Subjected to Combined Lateral and Gravity Loads," *ACI Structural Journal*, V. 94, No. 6, Nov.-Dec. 1997, pp. 723-729.
9. Darvall, P., and Allen, F., "Lateral Load Effective Width of Flat Plates with Drop Panels," *ACI JOURNAL, Proceedings* V. 81, No. 6, Nov.-Dec. 1984, pp. 613-617.
10. Dovich, L. M., and Wight, J. K., "Lateral Response of Nonseismically Detailed Reinforced Concrete Flat Slab Structures," *Report No. UMCEE 94-30*, Department of Civil and Environmental Engineering, University of Michigan, Ann Arbor, Mich., Sept. 1994, 183 pp.
11. Dovich, L. M., and Wight, J. K., "Lateral Behavior of Older Flat Slab Frames and the Economic Effect on Retrofit," *Earthquake Spectra*, EERI, V. 12, No. 4, Nov. 1996, pp. 667-691.
12. Kanaan, A. E., and Powell, G. H., "DRAIN-2D, A General Purpose Computer Program for Inelastic Dynamic Response of Plane Structures," *Report No. EERC 73-6*, Earthquake Engineering Research Center, University of California, Berkeley, Calif., Apr. 1973, 84 pp.
13. Tang, X., and Goel, S. C., "DRAIN-2DM Technical Notes and User's Guide," *Research Report UMCE 88-1*, Department of Civil Engineering, University of Michigan, Ann Arbor, Mich., Jan. 1988.
14. Naaman, A. E., *Prestressed Concrete Analysis and Design*, McGraw-Hill, Inc., New York, 1982, p. 448.
15. Singh, J. P.; Donovan, N. C.; and Jobnis, A. C., "Design of Machine Foundations on Piles," *Journal of the Geotechnical Engineering Division*, ASCE, V. 103, No. 8, Aug. 1977, pp. 79-111.
16. International Conference of Building Officials, "Uniform Building Code," V. 2, Los Angeles, Calif., 1997, 492 pp.
17. Diebold, J. W., and Moehle, J. P., "Lateral Load Response of Flat Plate Frames," *Journal of Structural Engineering*, ASCE, V. 111, No. 10, Oct. 1985, pp. 2149-2164.
18. Hall, J. F., ed., "Northridge Earthquake—Jan. 17, 1994, Preliminary Reconnaissance Report," *Report No. EERI 94-01*, Earthquake Engineering Research Institute, Oakland, Calif., Mar. 1994, 96 pp.